



} Faculté de médecine

Année 2017/2018

N°

Thèse

Pour le

DOCTORAT EN MEDECINE

Diplôme d'État

par

Antoine BRAULT

Né(e) le 31/08/1987 à Paris (75)

DWI MR imaging: can we improve the characterization of adnexal masses.

Présentée et soutenue publiquement le **30/10/2018** devant un jury composé de :

Président du Jury : Professeur Laurent BRUNEREAU, Radiologie et Imagerie Médicale, Faculté de Médecine – Tours

Membres du Jury :

Professeur Frédéric PATAT, Biophysique et Médecine Nucléaire, Faculté de Médecine – Tours

Docteur Aurore BLEUZEN, Radiodiagnostic et Imagerie Médicale, PH, CHRU – Tours

Directeur de thèse : Professeur Isabelle THOMASSIN-NAGGARA, Radiodiagnostic et Imagerie Médicale, Faculté de Médecine Pierre et Marie Curie - Paris

Titre: Imagerie IRM de Diffusion : peut-on améliorer la caractérisation des masses annexielles

RESUME

Objectif: Evaluer les différents paramètres ADC (moyenne, minimum, maximum, déviation standard et percentiles) issus d'une région d'intérêt localisée et d'une région d'intérêt occupant la plus grande partie possible de la portion solide de tumeurs ovariennes bénignes, frontières et malignes. Nous avons également essayé d'associer une valeur quantitative issue de la cartographie ADC au Score ADNEX-MR pour prédire le potentiel invasif d'une tumeur ovarienne.

Matériels et méthodes: 194 femmes (âge médian de 53,5 ans, de 18 à 95 ans) représentant 240 lésions ovariennes ont été incluses dans notre étude. Elles ont bénéficié d'une IRM pelvienne avec une séquence de diffusion. Deux radiologues experts ont relu les examens évaluant les lésions selon le score ADNEX-MR. Un radiologue junior a dessiné 2 régions d'intérêt (une petite localisée et une la plus grande possible) dans la portion tissulaire des masses annexielles. Les valeurs moyennes, minimales, maximales, la deviation standard pour les 2 régions d'intérêt ont été calculées pour les différentes lésions ainsi que les 5ème, 10ème, 20ème, 50ème, 75ème et 95ème percentiles pour la plus grande région d'intérêt, basées sur les constatations anatomopathologiques et le suivi à 2 ans. Les tests exact de Fisher, du Chi², de Kruskal-Wallis, de Mann-Whitney et l'analyse de courbes ROC ont été effectués pour l'analyse statistique.

Résultats: Les valeurs d'ADC moyennes, minimales et maximales dans les portions solides des tumeurs ovariennes sont significativement plus faibles dans les tumeurs invasives que dans les tumeurs frontières et bénignes quelque soit le type de région d'intérêt utilisé. Les 10ème, 20ème, 50ème 75ème et 95ème percentiles de la valeur des coefficients d'ADC de la région d'intérêt la plus large étaient également significativement plus faible dans les tumeurs invasives que dans les tumeurs bénignes ou frontières.

Title : DWI MR imaging: can we improve the characterization of adnexal masses.

ABSTRACT

Purpose: To assess different ADC values (as mean, minimum, maximum and standard deviation) in a larger population, from an hotspot and a larger area region of interest (ROI) drawn in the tissular portion from benign, borderline and invasive ovarian lesions. Besides we tried to add quantitative ADC value to ADNEXMR Score to predict invasiveness of an ovarian tumor.

Material and methods: One hundred and ninety four women (median age, 53,5 years, 18-95 years) with 240 lesions (151 women had a unique mass, 40 had two masses, on the same ovary or bilateral lesion, 3 women had 3 lesions) were included in our study and underwent MR scan with Diffusion Weighted sequence. Two senior radiologist reviewed images and scored MR results according to previously A_{DNEX}MR-Score. A junior radiologist drew two ROI (hotspot and a larger one) in the tissular portion of the adnexal masses. Mean, standard deviation, minimum and maximum values, 5th, 10th, 20th, 50th, 75th, 95th percentiles on ADC Map were computed for each ROI according to surgical histopathology or two-years follow-up findings. Statistical analysis was performed by using Fischer exact, chi-squared, Kruskal-Wallis, and Mann Whitney tests and ROC analysis.

Results: Mean, minimum and maximum ADC values in ovarian solid portion are lower in invasive tumors than in benign and borderline tumors whatever the ROI used (Hotspot or a larger area). The 10th, 20th, 50th, 75th, 95th percentiles ADC coefficient from the larger area ROI were also lower in invasive tumors than in benign or borderline masses. The maximum ADC value from the hotspot ROI was the best parameters to distinguish malignant from benign lesions and invasive from non-invasive lesions with an optimum cut-off point was respectively, a hotspot maximum ADC value $\leq 1.03 \times 10^{-3} \text{ mm}^2/\text{s}$ and $\leq 1 \times 10^{-3} \text{ mm}^2/\text{s}$ with a PLRMalignant = 2.07 and PLRInvasiveness = 2.65. In the sub-group rated ADNEX-MRSCORE 4 or 5, a hotspot maximum ADC value $\leq 1.04 \times 10^{-3} \text{ mm}^2/\text{s}$ are more likely to be invasive with a PLRInvasiveness = 3.3.

Conclusion: Ovarian tumors with a tissular portion with a low maximum ADC are more likely to be malignant (invasive and borderline) or invasive tumors. But this is not accurate enough to distinguish malignant from borderline or invasive from non-invasive without using morphological and contrast-enhancement sequence

Mot-clés: Tumeurs ovariennes, diffusion, coefficient ADC, masses, caractérisation

Key Words: Ovarian, tumors, DWI, ADC, MR, masses, characterization

UNIVERSITE DE TOURS
FACULTE DE MEDECINE DE TOURS

DOYEN

Pr Patrice DIOT

VICE-DOYEN

Pr Henri MARRET

ASSESSEURS

Pr Denis ANGOULVANT, Pédagogie

Pr Mathias BUCHLER, Relations internationales

Pr Hubert LARDY, Moyens – Relations avec l’Université

Pr Anne-Marie LEHR-DRYLEWICZ, Médecine générale

Pr François MAILLOT, Formation Médicale Continue

Pr Patrick VOURC’H, Recherche

RESPONSABLE ADMINISTRATIVE

Mme Fanny BOBLETER

DOYENS HONORAIRES

Pr Emile ARON (†) – 1962-1966

Directeur de l’Ecole de Médecine - 1947-1962

Pr Georges DESBUQUOIS (†) - 1966-1972

Pr André GOUAZE - 1972-1994

Pr Jean-Claude ROLLAND – 1994-2004

Pr Dominique PERROTIN – 2004-2014

PROFESSEURS EMERITES

Pr Daniel ALISON

Pr Philippe ARBEILLE

Pr Catherine BARTHELEMY

Pr Christian BONNARD

Pr Philippe BOUGNOUX

Pr Alain CHANTEPIE

Pr Pierre COSNAY

Pr Etienne DANQUECHIN-DORVAL

Pr Loïc DE LA LANDE DE CALAN

Pr Alain GOUDÉAU

Pr Noël HUTEN

Pr Olivier LE FLOC'H

Pr Yvon LEBRANCHU

Pr Elisabeth LECA

Pr Anne-Marie LEHR-DRYLEWICZ
Pr Gérard LORETTE
Pr Roland QUENTIN
Pr Alain ROBIER
Pr Elie SALIBA

PROFESSEURS HONORAIRES

P. ANTHONIOZ – A. AUDURIER – A. AUTRET – P. BAGROS – P. BARDOS – J.L. BAULIEU – C. BERGER – JC. BESNARD – P. BEUTTER – P. BONNET – M. BROCHIER – P. BURDIN – L. CASTELLANI – B. CHARBONNIER – P. CHOUTET – T. CONSTANS – C. COUET – J.P. FAUCHIER – F. FETISOF – J. FUSCIARDI – P. GAILLARD – G. GINIES – A. GOUAZE – J.L. GUilmot – M. JAN – J.P. LAMAGNERE – F. LAMISSE – Y. LANSON – J. LAUGIER – P. LECOMTE – E. LEMARIE – G. LEROY – Y. LHUINTRE – M. MARCHAND – C. MAURAGE – C. MERCIER – J. MOLINE – C. MORAINA – J.P. MUH – J. MURAT – H. NIVET – L. POURCELOT – P. RAYNAUD – D. RICHARD-LENOBLE – J.C. ROLLAND – D. ROYERE – A. SAINDELLE – J.J. SANTINI – D. SAUVAGE – D. SIRINELLI – B. TOUMIEUX – J. WEILL

PROFESSEURS DES UNIVERSITES - PRATICIENS HOSPITALIERS

ANDRES Christian Biochimie et biologie moléculaire
ANGOULVANT Denis Cardiologie
AUPART Michel Chirurgie thoracique et cardiovasculaire
BABUTY Dominique Cardiologie
BALLON Nicolas Psychiatrie ; addictologie
BARILLOT Isabelle Cancérologie ; radiothérapie
BARON Christophe Immunologie
BEJAN-ANGOULVANT Théodora Pharmacologie clinique
BERNARD Anne Cardiologie
BERNARD Louis Maladies infectieuses et maladies tropicales
BLANCHARD-LAUMONNIER Emmanuelle Biologie cellulaire
BLASCO Hélène Biochimie et biologie moléculaire
BODY Gilles Gynécologie et obstétrique
BONNET-BRILHAULT Frédérique Physiologie
BRILHAULT Jean Chirurgie orthopédique et traumatologique
BRUNEREAU Laurent Radiologie et imagerie médicale
BRUYERE Franck Urologie
BUCHLER Matthias Néphrologie
CALAIS Gilles Cancérologie, radiothérapie
CAMUS Vincent Psychiatrie d'adultes
CHANDENIER Jacques Parasitologie, mycologie
COLOMBAT Philippe Hématologie, transfusion
CORCIA Philippe Neurologie
COTTIER Jean-Philippe Radiologie et imagerie médicale
DE TOFFOL Bertrand Neurologie
DEQUIN Pierre-François..... Thérapeutique
DESOUBEAUX Guillaume..... Parasitologie et mycologie
DESTRIEUX Christophe Anatomie
DIOT Patrice Pneumologie
DU BOUEXIC de PINIEUX Gonzague Anatomie & cytologie pathologiques
DUCLUZEAU Pierre-Henri Endocrinologie, diabétologie, et nutrition
DUMONT Pascal Chirurgie thoracique et cardiovasculaire
EL HAGE Wissam Psychiatrie adultes
EHRMANN Stephan Réanimation

FAUCHIER Laurent Cardiologie
FAVARD Luc Chirurgie orthopédique et traumatologique
FOUGERE Bertrand Gériatrie
FOUQUET Bernard Médecine physique et de réadaptation
FRANCOIS Patrick Neurochirurgie
FROMONT-HANKARD Gaëlle Anatomie & cytologie pathologiques
GAUDY-GRAFFIN Catherine Bactériologie-virologie, hygiène hospitalière
GOGA Dominique Chirurgie maxillo-faciale et stomatologie
GOUPILLE Philippe Rhumatologie
GRUEL Yves Hématologie, transfusion
GUERIF Fabrice Biologie et médecine du développement et de la reproduction
GUYETANT Serge Anatomie et cytologie pathologiques
GYAN Emmanuel Hématologie, transfusion
HAILLOT Olivier Urologie
HALIMI Jean-Michel Thérapeutique
HANKARD Régis Pédiatrie
HERAULT Olivier Hématologie, transfusion
HERBRETEAU Denis Radiologie et imagerie médicale
HOURIOUX Christophe Biologie cellulaire
LABARTHE François Pédiatrie
LAFFON Marc Anesthésiologie et réanimation chirurgicale, médecine d'urgence
LARDY Hubert Chirurgie infantile
LARIBI Saïd Médecine d'urgence
LARTIGUE Marie-Frédérique Bactériologie-virologie
LAURE Boris Chirurgie maxillo-faciale et stomatologie
LECOMTE Thierry Gastroentérologie, hépatologie
LESCANNE Emmanuel Oto-rhino-laryngologie
LINASSIER Claude Cancérologie, radiothérapie
MACHET Laurent Dermato-vénérérologie
MAILLOT François Médecine interne
MARCHAND-ADAM Sylvain Pneumologie
MARRET Henri Gynécologie-obstétrique
MARUANI Annabel Dermatologie-vénérérologie
MEREGHETTI Laurent Bactériologie-virologie ; hygiène hospitalière
MORINIÈRE Sylvain Oto-rhino-laryngologie
MOUSSATA Driffa Gastro-entérologie
MULLEMAN Denis Rhumatologie
ODENT Thierry Chirurgie infantile
OUAISSI Mehdi Chirurgie digestive
OULDAMER Lobna Gynécologie-obstétrique
PAGES Jean-Christophe Biochimie et biologie moléculaire
PAINTAUD Gilles Pharmacologie fondamentale, pharmacologie clinique
PATAT Frédéric Biophysique et médecine nucléaire
PERROTIN Dominique Réanimation médicale, médecine d'urgence
PERROTIN Franck Gynécologie-obstétrique
PISELLA Pierre-Jean Ophtalmologie
PLANTIER Laurent Physiologie
REMERAND Francis Anesthésiologie et réanimation, médecine d'urgence
ROINGEARD Philippe Biologie cellulaire
ROSSET Philippe Chirurgie orthopédique et traumatologique
RUSCH Emmanuel Epidémiologie, économie de la santé et prévention

SAINT-MARTIN Pauline Médecine légale et droit de la santé
SALAME Ephrem Chirurgie digestive
SAMIMI Mahtab Dermatologie-vénérérologie
SANTIAGO-RIBEIRO Maria Biophysique et médecine nucléaire
THOMAS-CASTELNAU Pierre Pédiatrie
TOUTAIN Annick Génétique
VAILLANT Loïc Dermato-vénérérologie
VELUT Stéphane Anatomie
VOURC'H Patrick Biochimie et biologie moléculaire
WATIER Hervé Immunologie

PROFESSEUR DES UNIVERSITES DE MEDECINE GENERALE

LEBEAU Jean-Pierre

PROFESSEURS ASSOCIES

MALLET Donatien Soins palliatifs
POTIER Alain Médecine Générale
ROBERT Jean Médecine Générale

MAITRES DE CONFERENCES DES UNIVERSITES - PRATICIENS HOSPITALIERS

BAKHOS David Physiologie
BARBIER Louise Chirurgie digestive
BERHOUET Julien Chirurgie orthopédique et traumatologique
BERTRAND Philippe Biostat., informatique médical et technologies de communication
BRUNAULT Paul Psychiatrie d'adultes, addictologie
CAILLE Agnès Biostat., informatique médical et technologies de communication
CLEMENTY Nicolas Cardiologie
DOMELIER Anne-Sophie Bactériologie-virologie, hygiène hospitalière
DUFOUR Diane Biophysique et médecine nucléaire
FAVRAIS Géraldine Pédiatrie
FOUQUET-BERGEMER Anne-Marie Anatomie et cytologie pathologiques
GATAULT Philippe Néphrologie
GOUILLEUX Valérie Immunologie
GUILLON Antoine Réanimation
GUILLON-GRAMMATICO Leslie Epidémiologie, économie de la santé et prévention
HOARAU Cyrille Immunologie
IVANES Fabrice Physiologie
LE GUELLEC Chantal Pharmacologie fondamentale, pharmacologie clinique
MACHET Marie-Christine Anatomie et cytologie pathologiques
MOREL Baptiste Radiologie pédiatrique
PIVER Éric Biochimie et biologie moléculaire
REROLLE Camille Médecine légale
ROUMY Jérôme Biophysique et médecine nucléaire

SAUTENET Bénédicte Néphrologie
TERNANT David Pharmacologie fondamentale, pharmacologie clinique
ZEMMOURA Ilyess Neurochirurgie

MAITRES DE CONFERENCES DES UNIVERSITES

AGUILLOH-HERNANDEZ Nadia Neurosciences
BOREL Stéphanie Orthophonie
DIBAO-DINA Clarisse Médecine Générale
MONJAUZE Cécile Sciences du langage - orthophonie
PATIENT Romuald Biologie cellulaire
RENOUX-JACQUET Cécile Médecine Générale

MAITRES DE CONFERENCES ASSOCIES

RUIZ Christophe Médecine Générale
SAMKO Boris Médecine Générale

CHERCHEURS INSERM - CNRS - INRA

BOUAKAZ Ayache Directeur de Recherche INSERM – UMR INSERM 1253
CHALON Sylvie Directeur de Recherche INSERM – UMR INSERM 1253
COURTY Yves Chargé de Recherche CNRS – UMR INSERM 1100
DE ROCQUIGNY Hugues Chargé de Recherche INSERM – UMR INSERM 1259
ESCOFFRE Jean-Michel Chargé de Recherche INSERM – UMR INSERM 1253
GILOT Philippe Chargé de Recherche INRA – UMR INRA 1282
GOUILLEUX Fabrice Directeur de Recherche CNRS – UMR CNRS 7001
GOMOT Marie Chargée de Recherche INSERM – UMR INSERM 1253
HEUZE-VOURCH Nathalie Chargée de Recherche INSERM – UMR INSERM 1100
KORKMAZ Brice Chargé de Recherche INSERM – UMR INSERM 1100
LAUMONNIER Frédéric Chargé de Recherche INSERM - UMR INSERM 1253
LE PAPE Alain Directeur de Recherche CNRS – UMR INSERM 1100
MAZURIER Frédéric Directeur de Recherche INSERM – UMR CNRS 7001
MEUNIER Jean-Christophe Chargé de Recherche INSERM – UMR INSERM 1259
PAGET Christophe Chargé de Recherche INSERM – UMR INSERM 1100
RAOUL William Chargé de Recherche INSERM – UMR CNRS 7001
SI TAHAR Mustapha Directeur de Recherche INSERM – UMR INSERM 1100
WARDAK Claire Chargée de Recherche INSERM – UMR INSERM 1253

CHARGES D'ENSEIGNEMENT

Pour l'Ecole d'Orthophonie

DELORE Claire Orthophoniste
GOUIN Jean-Marie Praticien
Hospitalier PERRIER Danièle Orthophoniste

Pour l'Ecole d'Orthoptie

LALA Emmanuelle Praticien Hospitalier
MAJZOUB Samuel..... Praticien Hospitalier

Pour l'Ethique Médicale

BIRMELE Béatrice Praticien Hospitalier

SERMENT D'HIPPOCRATE

En présence des Maîtres de cette
Faculté, de mes chers condisciples
et selon la tradition d'Hippocrate,
je promets et je jure d'être fidèle aux lois de l'honneur
et de la probité dans l'exercice de la Médecine.

Je donnerai mes soins gratuits à l'indigent, et
n'exigerai jamais un salaire au-dessus de mon travail.

Admis dans l'intérieur des maisons, mes yeux
ne verront pas ce qui s'y passe, ma langue
taira

les secrets qui me seront confiés et mon état ne servira
pas à corrompre les mœurs ni à favoriser le crime.

Respectueux et reconnaissant envers mes
Maîtres, je rendrai à leurs enfants
l'instruction que j'ai reçue de leurs pères.

Que les hommes m'accordent leur
estime si je suis fidèle à mes promesses.

Que je sois couvert
d'opprobre et méprisé de
mes confrères si j'y
manque.

Remerciements

Aux membres du Jury :

Au Pr. Isabelle THOMASSIN-NAGGARA qui m'a fait l'honneur de bien vouloir diriger ce travail. Merci pour ton aide dans l'élaboration de ce travail et pour m'avoir aidé à tenir un timing serré.

Au Pr. Laurent BRUNEREAU, merci pour tout ce que vous m'avez appris au cours de mon stage à Troussseau, pour votre bienveillance. Je suis honoré que vous soyez le président de mon jury de thèse.

Au Pr. Frédéric PATAT, de m'avoir accueilli à plusieurs reprises dans vos services. J'ai toujours plaisir à discuter avec vous, vous m'avez toujours soutenu et pour cela, je vous en suis très reconnaissant.

Au Dr. Aurore BLEUZEN, tu m'as initié à l'imagerie de la Femme et notamment l'échographie pelvienne. Ta rigueur et ta passion pour la radiologie m'ont toujours beaucoup impressionné. Merci de m'avoir transmis le « virus ».

Merci également,

Au Pr. COTTIER, de m'avoir aidé et soutenu tout au long de mon internat.

Aux Dr ROULOT, ROUMY, BESSON, SCOTTO, pour tout ce que vous m'avez appris, pour votre gentillesse et votre bonne humeur.

Au service de Radiologie Générale et de Neuroradiologie d'Orléans, équipe médicale et para-médicale, qui m'avez beaucoup appris et permis d'arriver serein au « CHU ».

A l'équipe de Sénologie de Bretonneau, en particulier au Dr. VILDE pour tout ce que tu m'as appris et pour ta confiance.

A l'équipe de Radiologie de TENON, en particulier au Pr. BOUDGHENE pour m'avoir accueilli dans votre service. Au Pr. BAZOT pour votre enthousiasme communicatif et votre gentillesse. Et surtout au Dr. CHOPIER, pour m'avoir tant appris lors de nos vacations partagées à l'IRM, en séno interventionnelle et diagnostique.

A mes chefs préférés : Dr. CAYET, BURASCHI, DEROT, DEJOBERT, DEE, ACIU, DOMINTE, PUCHEUX, GEFFRAY, CAZENEUVE. Travailler avec vous a été un pur bonheur.

A mes co-internes que ce soit à Tours ou à Orléans, pour la bonne ambiance quelque soit les stages.

A mes amis, Jimmy, Mika, Nico, Julien, Laura, Pauline, Hugues, Doris, David, Clara, Valérie, Maxime, Rockeur, Salim, Julien dit « le hollandais volant » que ce soit au collège, lycée, pendant l'externat, l'internat, sans vous, ces années d'études n'auraient pas été les mêmes. J'espère que nos liens resteront les mêmes.

A ma famille :

Tiphaine, merci de m'avoir supporté tout au long de ces études, de toujours avoir eu confiance en moi. Tu as toujours été là, même dans les moments les plus difficiles. Maintenant que nous sommes 3 avec notre petite Romane, j'ai hâte de voir notre petite famille évoluer. Je vois l'avenir sereinement avec toi.

A mes frères, Thomas et François, et mon meilleur ami-frère, Alexis, vous êtes géniaux. Je suis tellement heureux de vous avoir. Que la vie nous permette de nous retrouver souvent autour de bons repas pour refaire le monde jusqu'au bout de la nuit.

A ma marraine, François, Alain, Maïdo, vous allez pouvoir arrêter de me demander « mais tu en es où maintenant ? » à chaque fois que l'on se voit. Merci à Bernard et Freddy de m'avoir accueilli au début de mon internat.

A ma belle famille, pour m'avoir si bien accueilli parmi vous.

A mon père, qui a toujours fait ce qui était le mieux pour moi dans la vie. Même si je ne te le dis pas, tu es un exemple. Merci.

A mes grands-parents, qui ont été très aimants, j'ai tellement de bons souvenirs. Je ne vous oublierai pas.

Et pour finir, je veux remercier ma mère. Elle m'a toujours soutenu, écouté, consolé, réconforté. Tu n'as jamais douté de mes choix, je pouvais tout te dire. Tu me manques terriblement tous les jours. J'espère que de là où tu es, tu es fière de moi.

Table des matières

INTRODUCTION	15
MATERIAL AND METHODS	16
Population	17
MR acquisition.....	21
MR Data Analysis.....	23
Morphological analysis.....	23
Functional Analysis.....	24
Reference standard	26
Statistical analysis.....	26
RESULTS.....	27
DESCRIPTIVE ANALYSIS.....	27
Morphological characteristics	27
ADNEXMR SCORE Analysis	28
QUANTITATIVE DWI MR analysis	31
Benign versus Invasive tumors	32
Benign versus Borderline tumors	33
Borderline versus Invasive Tumors	33
Benign versus Malignant	33
Non-Invasive versus Invasive.....	35
ADDED VALUE OF DWI MR PARAMETERS TO ADNEXMR SCORE	37
A _{DNEX} MR-S _{CORING} 4 or 5.....	37
DISCUSSION	39
ANNEXES.....	46
Annexe 1: ADNEX MR Score	46
Annexe 2 : Lexicon.....	47

INTRODUCTION

Adnexal masses are the first indication for gynecologic surgery [1] (Curtin JP).

Among those masses, ovarian neoplasms are often asymptomatic during the initial stage of the disease, that is why the diagnosis are often made in an advanced stage, with a bad prognosis and explains why ovarian tumors are called "silent killer" [2] (Le Page C). Ovarian tumors characterization is a challenge for radiologists. Indeed, as ovaries are located deeply in the pelvis, biopsies cannot easily be performed. Thus, pre-operative diagnosis is a key to manage accurately the patient. In particular, the aim is to avoid unnecessary surgery for patients who had a benign or eventually borderline lesions where oncologic and fertility preservation options could be discussed for young patients in expert centers. Besides, for malignant tumors an appropriate surgical procedure with most complete resection is one of the most important prognostic factor [3] (Bristow RE).

To diagnose ovarian lesions, ultrasonography (US) is the first line exam [4] (Gynecologic sonography: report) but has well-known limitations in particular for complex adnexal masses [5] (Kinkel K). In second line, Magnetic Resonance Imaging (MRI) using morphological sequences is more accurate than US for discriminate complex benign ovarian lesions from malignant with an accuracy from 83% to 93% [6] (Hricak H) [7] (Sohaib SA). Adding functional sequences helps to optimize adnexal masses characterization and Dynamic Contrast Enhanced sequence from 91 to 98% [8] (Thomassin-Naggara) with functional sequences as Diffusion Weighted sequence (DWI), and Dynamic Contrast Enhanced (DCE) [9] (Bernardin L)[10] (Dilks P). The A_{DNEX}MR Score using morphological, DWI and DCE sequences was created to help

radiologist to evaluate malignancy of an adnexal tumor [12] (Thomassin-Naggara I, Adnex MR score).

In addition to DWI sequence which is qualitative assessment on tissue cellularity and cell membrane integrity by detecting the extent of diffusion of free water molecules, the Apparent Diffusion Coefficient (ADC) provides a quantitative measurement of the diffusion of water molecules in tissues. Several studies have reported that ADC values from solid portion in differ among malignant, borderline, and benign ovarian tumors and can be useful for distinguishing malignant from benign or borderline ovarian tumors [12](Li W) [13](Zhao SH) [14] (Takeuchi). But these studies have included limited numbers of patients and reported varied diagnostic performances [15] (Kurata, Yasuhisa & Kido).

The purpose of our study was to assess different ADC values (as mean, minimum, maximum and standard deviation) in a larger population, from an hotspot and a larger area region of interest (ROI) drawn in the tissular portion from benign, borderline and invasive ovarian lesions. The 5th, 10th, 25th, 50th, 75th and 95th percentiles from larger area ROI were also evaluated. Besides we tried to add quantitative ADC value to A_{DNEX}MR Score to predict invasiveness of an ovarian tumor.

MATERIAL AND METHODS

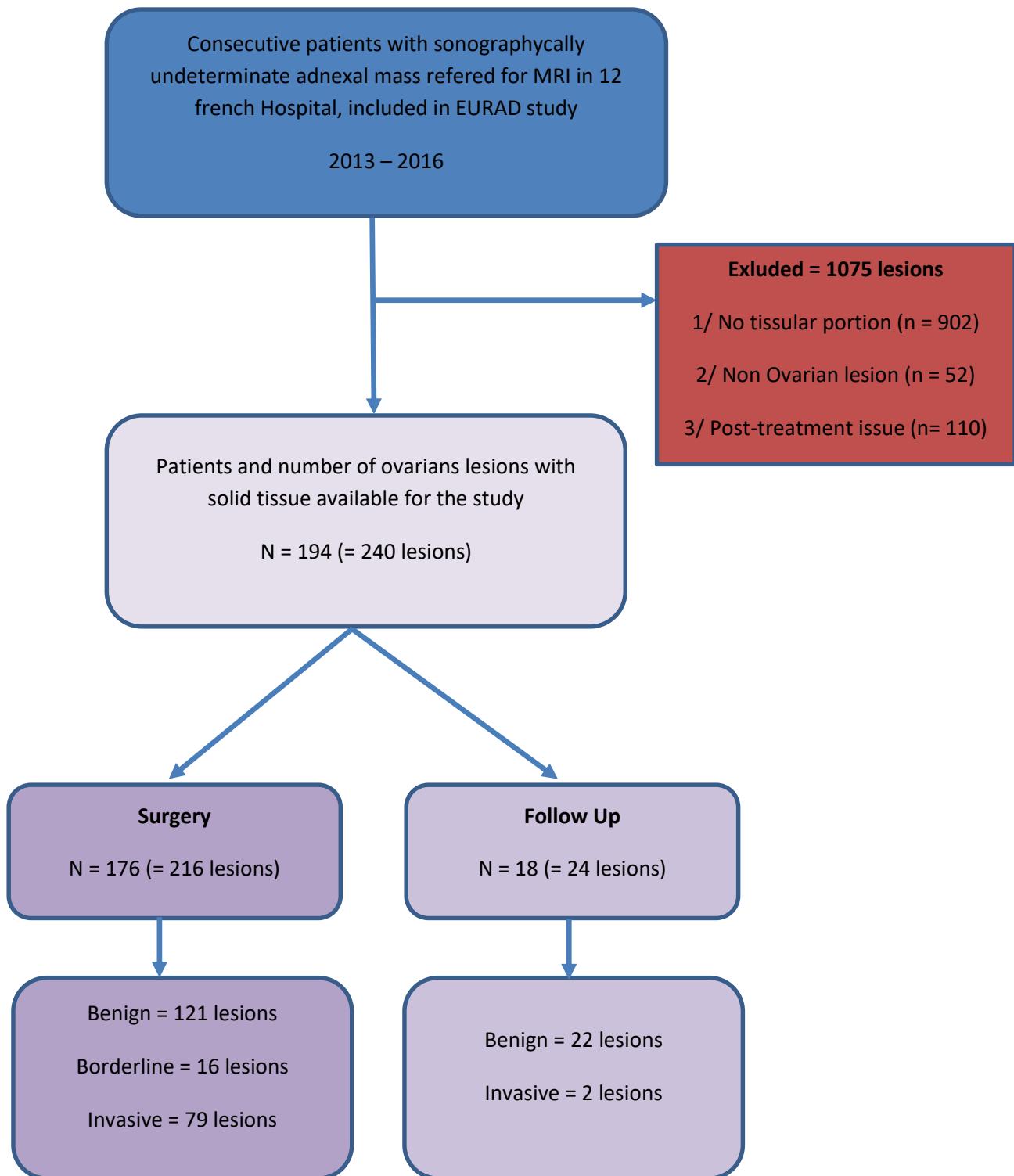
Institutional ethic committee approved the study. The population is issued from prospective data acquired in 12 centers from France (Tenon Hospital, Paris; Georges Pompidou European Hospital, Paris; Lariboisiere Hospital, Paris; Pitie-Salpetriere Hospital, Paris; Pyramides Imagery Center, Paris; Curie Institut, Paris; Gustave Roussy

Institut, Paris; La Timone Hospital, Marseille; Paoli Calmettes Institut, Marseille; Lapeyronie Hospital, Montpellier; Valenciennes Hospital, Valenciennes; Oscar Lambret Center, Valenciennes) participating in EURAD study clinical trial (CLINICAL TRIAL NCT01738789). All patients signed an informed consent.

Population

Between 2013/03/05 and 2016/03/31, all patients with sonographically indeterminate adnexal mass referred for MR imaging in our center were consecutively included in EURAD study. To be included, patients had to be more than 18 years old, with sonographically indeterminate adnexal mass, and had to have given their informed consent. Women who were pregnant, had any contra-indication to MR imaging (such as pace-maker, ferromagnetic material, or any other contra indication), had intolerance to gadolinium contrast agents or had severe renal insufficiency (GFR < 30 mL/min/1.73m²) were not included (Figure 1).

Figure 1 : Flowchart showing patient population and index test results.



Thus, 1006 patients have been prospectively included in 12 french centers representing 1328 lesions considered as complex adnexal masses on ultrasound exam. 902 lesions didn't show solid tissue (displaying a solid tissue as defined by Timmerman et al [16], including vegetation, solid portion, and thickened septa) and then were excluded. 52 lesions were excluded because considered as extra-ovarian lesions according 2 seniors reading conclusion. 110 lesions from Paoli-Calmettes Institut were excluded because of post treatment issue (non-loading of DCE MR sequences on workstation). Also, 11 more lesions were excluded for a solid tissue too small to draw a reliable ROI inside.

Thus, the final cohort consisted in 194 women (median age, 53,5 years, 18-95 years) with 240 lesions (151 women had a unique mass, 40 had 2 masses, on the same ovary or bilateral lesion, 3 women had 3 lesions).

176 patients, with 216 masses, underwent surgery. There were 24 cystectomies, 122 salpingo-oophorectomies (19 unilateral, 77 bilateral, and 26 non reported), 75 hysterectomies associated with salpingo-oophorectomies, 1 myomectomy (one broad ligament myoma) and 95 biopsies (hepatic, vaginal, antral or peritoneal). 18 patients underwent clinical or imaging follow-up.

Histopathological findings included 143 benign, 16 borderline and 81 invasive malignant lesions, are reported in Table 1.

Table 1: Reference Standard Findings

		Number of lesions n = 240
Bilateral		40
Three lesions by patient		3
Establishment of final diagnosis	Surgical pathology Follow-up (2 years or more)	216 24
Final diagnosis	BENIGN - Serous cystadenomas - Mucinous cystadenomas - Brenner tumor - Cystadenofibroma - Benign Germ Cell Tumor - Sex-cord tumors - Functional cyst - Mesothelial cyst - Myoma - Indeterminate (2 stable follow up and 2 disappeared) - Pelvic Inflammatory disease /Fibrosis - Adnexal Torsion - Hydrosalpinx	143 38 3 3 29 24 32 1 1 2 4 2 2 2 2
	BORDERLINE - Serous tumors	16 12

	- Mucinous tumors - Cystadenofibroma	2 2
	INVASIVE	81
	- Cystadenocarcinomas	32
	- Other epithelial carcinomas	18
	- Sex-cord stromal tumors	3
	- Metastases	21
	- Tubal cancers	3
	- Other (urothelial, neuroendocrine tumors...)	4

MR acquisition

MRI sequences were acquired at 1.5T (GE MR 450 W or GE Sigma HDX, Milwaukee, USA; or Philips ACHIEVA, Koninklijke, Netherlands; or Philips INTERA, Koninklijke, Netherlands; or Siemens AVANTO, Munich, Germany) or 3T (GE Discovery MR 750 or GE GEMS or GE SIGNA, Milwaukee, USA; or Siemens SKYRA, Munich, Germany). The patients were placed in a phased-array pelvic coil in the supine position with an intravenous (IV) access in place. All sequences were acquired with saturation bands placed anteriorly and posteriorly to eliminate the high signal from subcutaneous fat. The patients fasted for three hours and received an antispasmodic drug intravenously (1 mg of Glucagon Chlorhydrate, GLUCAGEN ; Novo Nordisk, France) immediately before MRI to reduce bowel peristalsis. A sagittal T2-weighted turbo spin-

echo sequence from one femoral head to the other (TR/TE 5280 msec/100.416 msec ; Flip angle 160° ; echo-train length 24; slice thickness 4 mm; gap 1 mm; field of view 24 cm; excitations 3; and matrix size 320x240), axial T2-weighted turbo spin-echo sequence from the renal hilum to the symphysis pubis (TR/TE 9926 msec/100.608 msec; Flip angle 160° ; echo-train length 24; slice thickness 5 mm; gap 1 mm; field of view 30 cm; excitations 1.5; and matrix size 320x240) and axial T1-weighted gradient-echo sequence (TR/TE 205/4.2; flip angle 12°; excitations 2 ; slice thickness 6mm; No gap; field of view 30 cm and interpolated matrix size 280 x240) were obtained. Diffusion-weighted MR images in the axial plane (TR/TE 10750 msec / Minimum; TI 89 msec ; number of shots 1 ; slice thickness 5 mm; gap 1 mm; field of view 38 cm and interpolated matrix size 120 x100) were systematically added. The b-values corresponding to the diffusion-sensitizing gradient were 0 and 1000 or 1200 seconds/mm². Motion-probing gradient pulses were placed in the three orthogonal planes.

DCE T1-weighted isotropic gradient-echo sequences (three dimensional [3D] Fast Spoiled Gradient-Recalled-Echo [FSPGR]) (Axial plan, TE Minimum; flip angle 30°; slice thickness 3 mm; no gap ; bandwith 62.5kMHz, excitation 1; field of view 35 x 31.5 ; and interpolated matrix size 256 x 180, 54 slices (i.e z=16.2cm)) were acquired. Gadolinium chelate (DOTAREM ; Guerbet, Aulnay, France) was given at a dose of 0.2 mL.kg⁻¹ via a Power Injector (Medrad, Maastricht, The Netherlands) at a rate of 2 mL.second⁻¹, followed by 30 mL of normal saline to flush the tubing. Images were obtained at 15-second intervals for 4 min 30, beginning 10 seconds before the bolus injection.

Finally, delayed post-contrast axial and sagittal T1-weighted gradient-echo images with breath hold were performed after gadolinium injection.

156 lesions were performed on 1.5T MRI and 84 lesions were performed on 3T.

All of the MR images were reviewed on a Osirix workstation and sent to OLEASPHERE 3.0 (La Ciotat, France) for DWI MR analysis.

MR Data Analysis

Two senior radiologists, with experience in pelvic MRI, independently reviewed MR images, informed of clinical and ultrasonographic data, but blinded to the histologic results or following.

Morphological analysis

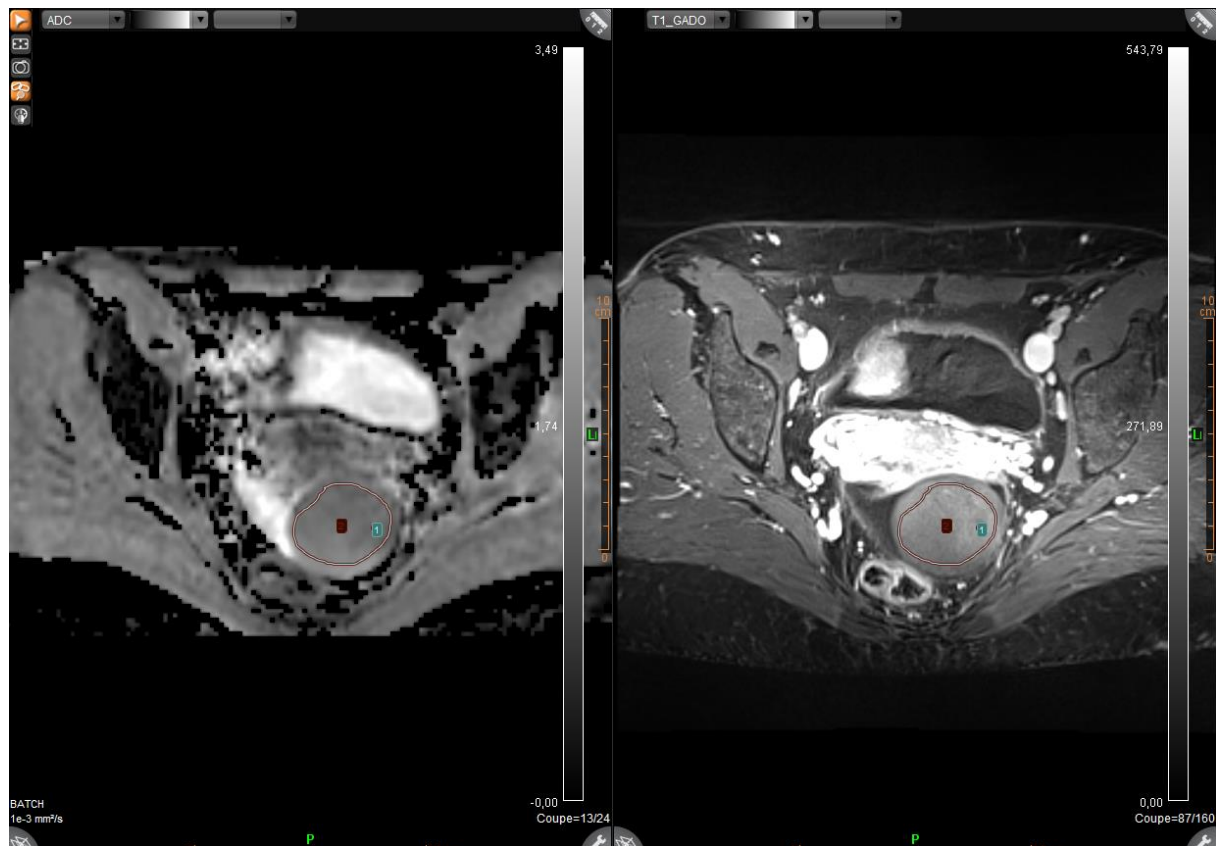
The following items were recorded: size, side and origin of the adnexal mass, bilaterality, wall enhancement, bi or multilocularity, type of solid tissue (solid portion, vegetation, thickened regular and irregular septa, grouped septa). When there were multiples masses, each lesion was analyzed. T2-weighted signal intensity within the solid tissue (low or intermediate compared with that of the outer myometrium) and b = 1000 or 1200 sec/mm²-weighted signal intensity within the solid tissue (high diffusion-weighted signal intensity compared with that of serous fluid; i.e. urine within bladder or cerebro-spinal fluid [CSF]) were analyzed. Finally, the presence of associated ascites and peritoneal implants was reported.

Functional Analysis

For dynamic contrast analysis, two regions of interest (ROIs) was drawn ; one in the external myometrium and one in solid tissue portion of the adnexal masse. The enhancement was classified using a previously published time intensity curve classification [17]. A gradual increase in the signal intensity of the solid tissue, without a well-defined "shoulder," was defined as curve type 1. A moderate initial increase in the signal intensity of solid tissue compared with that of the external myometrium, followed by a plateau, was defined as curve type 2. An initial increase in the signal intensity of solid tissue that was steeper than that of myometrium was defined as curve type 3. When patients underwent hysterectomy, time intensity curve with well-defined "shoulder" were classified as type 2 and without classified as type 1.

For diffusion analysis, the ADC values of each lesion was evaluated by drawing two ROI on ADC maps: one circular ROI (Hotspot) was placed visualy on the most enhanced area of the entire tissular portion (mean ROI size = 13.01 mm^2 , [IC 95%:10 – 16]), and an other larger ROI (Area) was hand-free drawed to be as large as possible (mean ROI size = 272.95 mm^2 , [IC 95%: 208 – 337]) within the confines of the tissular portion without involving artifact from tumour/air interface or blood flow (figure 2).

Figure 2 : Female patient with ovarian fibroma. Two region of interest are drawned. A circular one visually placed on the most enhanced area of the entire tissular portion and a larger one drawned to be as large as possible within the confines of the tissular portion without involving artifact from tumour/air interface or blood flow.



When the lesion was heterogeneous, the ROI was placed in order not to involve hemorrhage, necrosis or cystic components within the lesion by referring to conventional T1- and T2-weighted sequences. Then, OLEASPHERE computed mean, standard deviation, minimum and maximum values 5th, 10th, 20th, 50th, 75th, 95th percentiles.

Reference standard

Final diagnoses were established by means of surgical pathologic results for 176 patients (216 lesions) or based on 2-years clinical or imaging follow-up for 18 patients (24 lesions) (Table 1). Among the 24 lesions evaluated with clinical or imaging follow-up at 2 years, 3 resolved, 2 increased in size, 2 decreased and 17 were stable in size and appearance.

Statistical analysis

Descriptive analysis was performed by using the Chi² test and Fisher exact test for categorical parameters. Intraclass correlation coefficients were calculated on each DWI-MR continuous parameter estimated by hotspot ROIs or larger ROIs (mean, minimum, maximum, standard deviation values). Significant differences DWI MRI quantitative parameters according to the 3 histopathologic types (benign, borderline and invasive) were identified by using the nonparametric Kruskal-Wallis, a one-way analysis of variance by ranks. The null hypothesis of the Kruskal-Wallis test is that there is no difference in the medians of n populations, considering a set of n independent samples. When a significant result was found, we used Mann-Whitney test to compare samples 2 by 2, identify which of the histopathological groups were different and determine p -value. We used receiver operating characteristics curve (ROC) to determine the optimum cutoff point with the best sensitivity and specificity of the most relevant DWI-MR parameter for distinguishing malignant from non-malignant tumors in the entire population. Then we used ROC curve again to determine the optimum cutoff point with the best sensitivity and specificity of the most relevant

DWI-MR parameter for distinguishing invasive from non-invasive tumors in the A_{DNEX}MR-SCORING 4 or 5 population [11].

A *p*-value of less than 0.05 was considered statistically different. Statistical analyses were performed by using MedCalc software (MedCalc version 17.8 ; www.medcalc.be, Belgium).

RESULTS

DESCRIPTIVE ANALYSIS

Morphological characteristics (Table 2)

The presence of solid papillary projections was significantly more frequent in borderline than in benign ($p = 0,000001$) or invasive tumors ($p < 0,000001$) but no difference was observed between benign and invasive tumors. The presentation as solid portion in a mixed mass was more frequent in invasive than in benign tumors ($p = 0,004275$) and than in borderline tumors ($p = 0,03$), but no difference was found between benign and borderline tumors ($p = 0,593930$). The presentation as purely solid mass was more frequent in invasive than in borderline tumors ($p = 0,010632$) and in benign than in borderline tumors ($p = 0,013$) but no difference was found between benign and invasive tumors or benign or borderline tumors. No difference was found between benign, borderline or invasive groups about the presence of thickened irregular septa. Low T2W signal intensity of solid tissue was more frequent in benign than in borderline tumors ($p = 0,00002$) and in benign than in invasive tumors ($p < 0,000001$). Only one invasive or borderline tumors displayed low T2W

signal intensity of the solid tissue, it was an invasive tumor (metastasis). Low DW signal intensity of solid tissue was more frequent in benign than in borderline tumors ($p = 0,00002$) and in benign than in invasive tumors ($p < 0,000001$) but no difference was found between invasive and borderline tumors. Four of the invasive tumors displayed an intermediate or high DW signal intensity of the solid tissue (a mucinous and a serous cystadenocarcinoma, a endometriod carcinoma and a metastasis). Invasive tumors were bigger and had larger solid tissue than benign tumors ($p = 0,0012$ and $p < 0,0001$), and had larger solid tissue than borderline tumors ($p = 0,0002$). Borderline tumors were bigger than benign tumors ($p = 0,0034$). No difference was found in the size of tumors between invasive and borderline tumors nor in the size of solid tissue between borderline and benign tumors.

Time intensity curve Type 1 was more significantly more frequent in benign tumors than in borderline or invasive tumors (respectively $p= 0,00005$ and $p < 0,000001$). Time intensity curve Type 2 was more frequent in borderline tumors than in benign tumors ($p = 0,000013$) and than in invasive tumors ($p= 0,013$). Time intensity curve Type 3 was more frequent in invasive tumors than in benign tumors ($p= 0,0012$).

ADNEXMR SCORE Analysis

- $A_{DNEX}MR-Score$ 1, which means absence of pelvic mass on MR imaging, was not found in this study, because these cases were excluded from the study.
- $A_{DNEX}MR-Score$ 2, which corresponds to "Benign mass", represented in this study by lesions with solid tissue in lowT2W and low DW signal was found in 14.6% (35/240) with a $PLR_{malignancy} = 0$, as no malignant mass had a score 2.

- $A_{DNEX}MR-Score$ 3, which means “Probably benign mass”, represented in this study by lesions with solid tissue in intermediate T2W or high DW signal that enhances according a Time intensity curve type 1 was found in 28.7% (69/240) with a $PLR_{malignancy}= 0.067$. It was found in 66 benign, 2 borderline (serous and mucinous) and 1 malignant tumors (metastasis).
- $A_{DNEX}MR-Score$ 4, corresponding to “Indeterminate MR mass”, represented by lesions with solid tissue in intermediate T2W or high DW signal than enhances according a time intensity curve type 2 was found in 30% (72/240) with a $PLR_{malignancy}= 1.65$. It was found in 34 benign, 11 borderline and 27 invasive masses.
- $A_{DNEX}MR-Score$ 5, corresponding to “Probably malignant mass”, represented by lesions with solid tissue in intermediate T2W or high DW signal than enhances according a time intensity curve type 2 or lesions associated with peritoneal implants was found in 27% (64/240) with a $PLR_{malignancy}= 10.3$. There were 8 benign, 3 borderline and 53 invasive tumors. The 8 benign masses classified as $A_{DNEX}MR-Score$ 5 were two cystadenofibromas, 1 Brenner tumor and 5 mature teratomas.

Table 2: Morphological and enhancement features of the solid tissue of adnexal masses

	Benign (n=143)	Borderline (n=16)	Invasive (n=81)	p
Size of the tumor (mm) median/interquartile	47 (35 ;73.5)	80.5 (86.5 ;116.0)	84 (41.5 ;140)	0,000001
Size of the solid tissue in mixed masses (mm)	17 (9; 31.25)	22 (14.2; 27.5)	55 (36.2;80.7)	<0,000001
Papillary projection				
Present	44	15	22	< 0,0001
Absent	99	1	59	
Solid portion in a mixed mass				
Yes	58	5	50	= 0,0040
No	85	11	31	
Purely solid mass				
Yes	38	0	23	= 0,0515
No	105	16	58	
Thickened irregular septa				
Present	11	1	12	= 0,2037
Absent	132	15	69	
T2 weighted signal				
Low	75	0	1	< 0,0001
Intermediate or High	68	16	80	
DWI weighted signal				
Low	66	0	4	< 0,0001
Intermediate or High	77	16	77	
Time intensity curve				
Type 1	94	2	1	< 0,0001
Type 2	35	13	37	
Type 3	8	1	42	
Non feasible	6	0	1	
ADNEX MR Score				
Score 1	0	0	0	< 0,0001
Score 2	35	0	0	
Score 3	66	2	1	
Score 4	34	11	27	
Score 5	8	3	53	

P values were determined by Chi-squared test except for size for which P value was determined by

Kruskal-Wallis test

Overall accuracy of the score was 81.25% (195/240). Within the tumors classified A_{DNEX}MR-Score 1, 2 or 3, there were 2 borderline tumors (serous and mucinous) and 1 malignant tumor, a metastasis (i.e false negative). All the other ones were benign. The

$A_{DNEXMR-SCORING}$ 4 or 5 was found in 42 benign (i.e false positive), 14 borderline and 80 invasive masses including 27 invasive tumors classified as score 4. Then, in the sub-group including masses scored A_{DNEXMR} 4 or 5, $PLR_{Invasiveness} = 2.87$.

Hence, we worked to determine if it was possible to use quantitative ADC coefficient to improve the prediction of benign, borderline and invasive malignant subtypes with the score.

QUANTITATIVE DWI MR analysis

An excellent concordance of results between Hot Spot ROIs technique and Larger Area ROIs technique was found for mean, minimum and maximum values with Intra class coefficients (ICC) between 0.806 and 0.937 (Table 3).

Table 3: DCE MR parameters according ROI technique (Hotspot versus Larger Area)

	Intraclass Correlation Coefficient	95%CI
ADC mean	0,9373	[0,9202 ; 0,9508]
ADC max	0,8062	[0,7578 ; 0,8457]
ADC min	0,9118	[0,8882 ; 0,9306]
ADC STD	0,4674	[0,3643 ; 0,5593]

A poor to fair concordance was found for standard deviation parameter with ICC = 0,4674 (95% IC = [0,3643 ; 0,5593]).

Significant differences were found between benign, borderline and invasive tumors in all DWI MR parameters (mean, minimum, maximum, standard deviation, 5th, 10th, 20th, 50th, 75th, 95th percentiles) (table 4).

Table 4 : Comparison of ADC-DWI MRI parameters between benign, borderline and invasive adnexal tumors (median, percentile 25th, percentile 75th)

	Hotspot				Larger Area			
	Benign (n=143)	Borderline (n=16)	Invasive (n=81)	P*	Benign (n=143)	Borderline (n=16)	Invasive (n=81)	P*
ADC mean	1.07 (0.86;1.5)	1.25 (1.09;1.54)	0.84 (0.71;1.06)	<0,000001	1.170 (0.890;1.48)	1.370 (1.235;1.610)	0.960 (0.82;1.18)	0,000012
ADC min	0.99 (0.76;1.41)	1.195 (1;1.5)	0.78 (0.66;0.91)	0,000006	0.77 (0.48;1.16)	1.05 (0.78;1.4)	0.69 (0.57;0.82)	0,001167
ADC max	1.17 (0.98;1.58)	1.335 (1.155;1.615)	0.900 (0.80;1.165)	<0,000001	1.54 (1.21;1.92)	1.78 (1.56;2.005)	1.36 (1.147;1.552)	0,000090
ADC STD	0.06 (0.03;0.110)	0.05 (0.015;0.065)	0.04 (0.02;0.06)	0,004800	0.15 (0.12;0.21)	0.165 (0.115;0.190)	0.130 (0.09;0.163)	0,007245
ADC 5	-	-	-	-	0.83 (0.61;1.17)	1.110 (0.87;1.44)	0.75 (0.625;0.903)	0,001913
ADC 10	-	-	-	-	0.89 (0.67;1.24)	1.19 (0.955;1.445)	0.8 (0.675;0.94)	0,000314
ADC 20	-	-	-	-	0.99 (0.73;1.31)	1.235 (1.075;1.475)	0.840 (0.72;1.03)	0,000083
ADC 50	-	-	-	-	1.14 (0.89;1.55)	1.390 (1.23;1.6)	0.94 (0.79;1.18)	0,000009
ADC 75	-	-	-	-	1.31 (0.99;1.66)	1.495 (1.34;1.755)	1.04 (0.89;1.29)	0,000002
ADC 95	-	-	-	-	1.45 (1.15;1.87)	1.71 (1.495;1.94)	1.2 (1.04;1.44)	0,000001

* Kruskal-Wallis test

Benign versus Invasive tumors

Hotspot: Invasive tumors displayed significantly lower mean ADC coefficient, minimum ADC coefficient, maximum ADC coefficient and standard deviation ADC coefficient than benign tumors (p < 0,0001, p = 0,0001, p < 0,0001, p = 0,0014).

Larger Area: Invasive tumors displayed lower mean ADC coefficient, maximum ADC coefficient, standard deviation ADC coefficient, 10th, 20th, 50th, 75th, 95th percentiles ADC coefficient than benign tumors (p = 0,0008, p = 0,0018, p = 0,0025, p = 0,0365, p = 0,008, p = 0,0005, p = 0,0001, p < 0,0001).

Benign versus Borderline tumors

Hotspot: No significant difference was observed in mean ADC coefficient, minimum ADC coefficient, maximum ADC coefficient and standard deviation ADC coefficient, between benign and borderline tumors.

Larger Area: Borderline tumors displayed higher mean ADC coefficient, minimum ADC coefficient, maximum ADC coefficient than in benign tumors ($p = 0,022$, $p = 0,0179$, $p = 0,0492$).

Borderline versus Invasive Tumors

Hotspot: Invasive tumors displayed lower mean ADC coefficient, minimum ADC coefficient, maximum ADC coefficient than benign tumors ($p < 0,0001$, $p < 0,0001$, $p < 0,0001$).

Larger Area: Invasive tumors displayed lower mean ADC coefficient, minimum ADC coefficient, maximum ADC coefficient, 5th, 10th, 20th, 50th, 75th, 95th percentiles ADC coefficient than borderline tumors ($p < 0,0001$, $p < 0,0001$, $p < 0,0001$, $p = 0,0001$, $p < 0,0001$).

Benign versus Malignant (table 5)

Hotspot: Malignant tumors displayed lower mean ADC coefficient, minimum ADC coefficient, maximum ADC coefficient and STD ADC coefficient than benign tumors ($p = 0.0002$; $p = 0.0041$; $p < 0.0001$; $p = 0.0012$).

Larger Area: Malignant tumors displayed lower mean ADC coefficient, maximum ADC coefficient, STD ADC coefficient and lower 50th, 75th, 95th percentiles ADC

coefficient than benign tumors ($p= 0.286$; $p= 0.0351$; $p= 0.0078$; $p=0.0174$; $p= 0.0054$; $p= 0.004$).

Table 5 : Comparison of DWI MRI parameters and percentiles between benign and malignant adnexal tumors

ADC		Benign	Malignant	p*
Hotspot	Mean	1.07 (0.86;1.4975)	0.88 (0.7725;1.16)	0.0002
	Minimum	0.99 (0.76;1.4075)	0.82 (0.7175;1.075)	0.0041
	Maximum	1.17 (0.9825;1.5825)	0.95 (0.8175;1.2525)	<0.0001
	STD	0.06 (0.03;0.11)	0.04 (0.02;0.06)	0.0012
Larger Area	Mean	1.17 (0.89;1.48)	1.05 (0.85;1.2925)	0.0286
	Minimum	0.77 (0.48;1.16)	0.71 (0.6075;0.9025)	0.4634
	Maximum	1.54 (1.2125;1.925)	1.45 (1.17;1.6275)	0.0351
	STD	0.15 (0.12;0.21)	0.13 (0.10;0.1725)	0.0078
	5th percentiles	0.83 (0.61;1.1750)	0.78 (0.6775;0.985)	0,5066
	10th percentiles	0.89 (0.6725;1.245)	0.83 (0.71;1.0475)	0.3107
	25th percentiles	1.01 (0.7525;1.34)	0.94(0.7675;1.15)	0.0901
	50th percentiles	1.14 (0.89;1.545)	1.04 (0.8275;1.28)	0.0174
	75th percentiles	1.31 (0.985;1.655)	1.14 (0.91;1.36)	0.0054
	95th percentiles	1.45 (1.145;1.87)	1.3 (1.05;1.4925)	0.004

* Mann Whitney test

Non-Invasive versus Invasive (table 6)

Hotspot: Invasive tumors displayed lower mean ADC coefficient, minimum ADC coefficient, maximum ADC coefficient and STD ADC coefficient than non-invasive tumors ($p < 0,0001$; $p < 0,0001$; $p < 0,0001$; $p= 0.0023$).

Larger Area: Invasive tumors displayed lower mean ADC coefficient, minimum ADC coefficient, maximum ADC coefficient, STD ADC coefficient and lower 5th, 10th, 25th, 50th, 75th, 95th percentiles ADC coefficient than non-invasive tumors ($p= 0.0001$; $p= 0.015$; $p= 0.0002$; $p= 0.0017$; $p= 0.0209$; $p= 0.0048$; $p= 0.0004$; $p < 0.0001$; $p < 0.0001$; $p < 0.0001$).

Table 6 : Comparison of DWI MRI parameters and percentiles between non-invasive and invasive adnexal tumors

ADC	Parameters	Non Invasive	Invasive	P*
Hotspot	Mean	1.10 (0.88;1.5)	0.84 (0.715;1.075)	< 0,0001
	Minimum	1.02 (0.77;1.42)	0.78 (0.663;0.913)	< 0,0001
	Maximum	1.18 (1.002;1.600)	0.9 (0.798;1.165)	< 0,0001
	STD	0.05 (0.03;0.108)	0.04 (0.02;0.06)	0,0023
Larger Area	Mean	1.2 (0.91;1.498)	0.96 (0.823;1.18)	0,0001
	Minimum	0.81 (0.51;1.175)	0.690 (0.568;0.823)	0,0150
	Maximum	1.57 (1.245;1.937)	1.36 (1.147;1.552)	0,0002
	STD	0.15 (0.12;0.21)	0.13 (0.09;0.163)	0,0017
	5th percentiles	0.88 (0.643;1.2)	0.75 (0.625;0.903)	0,0209
	10th percentiles	0.9 (0.7;1.26)	0.8 (0.675;0.945)	0,0048
	25th percentiles	1.07 (0.8;1.35)	0.88 (0.733;1.07)	0,0004
	50th percentiles	1.19 (0.92;1.558)	0.94 (0.788;1.18)	< 0,0001
	75th percentiles	1.35 (1.04;1.67)	1.04 (0.89;1.29)	< 0,0001
	95th percentiles	1.5 (1.22;1.902)	1.2 (1.038;1.442)	< 0,0001

* Mann Whitney test

The optimum ADC parameter to distinguish malignant from benign tumors were Hotspot maximum ADC parameter according ROC curves (Area Under the Curve, AUC = 0,664) and a optimum cut-off ADC \leq 1,03 with a sensitivity = 60.8% and a specificity =70.6%. Using this criteria, among the 97 malignant tumors included in our study: 59 malignant tumors were correctly classified and 42 malignant tumors were misclassified. Thus, an adnexal tumor which had a Hotspot maximum ADC \leq 1,03 had a PLR_{Malignant} = 2,07.

The optimum ADC parameter to discriminate non-invasive from invasive tumors were Hotspot maximum ADC parameter according ROC curves (AUC = 0.729) and an optimum cut-off ADC value was \leq 1, with a sensitivity = 66.7% and a specificity =74.8%. With this ADC criteria, among the 81 invasive tumors included: 54 invasive tumors were correctly classified and 42 malignant tumors were misclassified. Thus, PLR_{Invasiveness}= 2.65.

ADDED VALUE OF DWI MR PARAMETERS TO ADNEXMR SCORE

ADNEXMR-SCORING 4 or 5

136 masses were scored AdnexMR 4 or 5 in our study including 56 non invasive adnexal tumors (42 benign masses and 14 borderline) and 80 invasives adnexal tumors.

Benign masses were including 9 serous tumors, 3 mucinous tumors, 1 Brenner tumor, 5 cystadenofibromas, 3 fibromas, 14 mature teratomas, 1 indeterminate tumor, 2 adnexal torsion, 2 hydrosalpinx/pelvic inflammatory disease.

Borderline masses were including 11 serous tumors, 1 mucinous tumor and 2 cystadenofibromas.

Invasive masses were including 31 serous tumors, 1 mucinous tumor, 10 clear cells tumors, 8 endometrioid tumors, 3 stromal and sexual tumors (1 Sertoli-Leydig and 2 granulosa), 20 metastasis and 7 others kind of tumors (1 mullerian adenocarcinoma, 3 tubal cancers, 1 urothelial cancer, 1 undifferentiated masse and 1 neuro-endocrine tumor).

In this population, all ADC parameters (mean, minimum, maximum, STD, 5th, 10th, 25th, 50th, 75th, 95th) from hotspot ROI or larger ROI were significantly lower in invasive masses than in non-invasive masses.

We performed ROC analysis in order to find the best parameter to discriminate invasive and non-invasive tumors. The Hotspot ADC maximum parameter was the one with the highest Area Under the Curve (0,774, IC95% [0,694, 0,841]). The optimum cut-off point was a maximum ADC ≤ 1.04 with 70% of sensitivity and 78.6% of specificity.

Adding this criteria to the A_{DNEX}MR Score 4 or 5, 68 masses were classified as invasive: 56 tumors were correctly identified as invasive. 12 non invasive masses were misclassified (2 benign serous tumors, 3 mature teratomas, 1 fibroma, 1 hydrosalpinx, 1 adnex torsion, 2 borderline cystadenofibromas, 1 borderline serous).

Thus, a masse rated A_{DNEX}MR Score ≥ 4 with an Hotspot maximum ADC ≤ 1.04 has a PLR_{Invasiveness} = 3,3.

DISCUSSION

Our study shows that mean, minimum and maximum ADC values in ovarian solid portion are lower in invasive tumors than in benign and borderline tumors whatever the ROI used (Hotspot or a larger area). The 10th, 20th, 50th, 75th, 95th percentiles ADC coefficient from the larger area ROI were also lower in invasive tumors than in benign or borderline masses.

The maximum ADC value from the hotspot ROI was the best parameters to distinguish malignant from benign lesions and invasive from non-invasive lesions with respectively a sensitivity = 60.8% and a specificity = 70.6% and a sensitivity = 66.7% and a specificity = 74.8%. The optimum cut-off point was respectively, a hotspot maximum ADC value $\leq 1.03 \times 10^{-3} \text{ mm}^2/\text{s}$ and $\leq 1 \times 10^{-3} \text{ mm}^2/\text{s}$ with a PLR_{Malignant} = 2.07 and PLR_{Invasiveness} = 2.65.

In addition to the A_{DNEX}MR Score, the ovarian lesions which was rated as A_{DNEX}MR Score 4 or 5 with a hotspot maximum ADC value $\leq 1.04 \times 10^{-3} \text{ mm}^2/\text{s}$ are more likely to be invasive with 70% of sensitivity, 78.6% of specificity and a PLR_{Invasiveness} = 3.3.

Diffusion Weighted Images (DWI) can be evaluated in two ways, qualitatively, by visual assessment of signal intensity, and quantitatively, by measurement of the apparent diffusion coefficient (ADC). The ADC value quantifies water proton motion, which in particular case of biological tissues this is an association of true water diffusion and capillary perfusion. The ADC value can theoretically be used to characterise tissues, as the degree of diffusion is correlated to cellular density and extracellular space volume [19][20]. Because ADC is related to the molecular translational

movement of water molecules, increased tissue cellularity or cell density decreases ADC value [21][22].

In ovarian lesions, DWI has been widely studied in several reports and is useful to detect invasive tissular portion in a complex adnexal mass [23][24][25]. But DWI can also be used to assess benignity if it is associated with morphological criteria : indeed an ovarian tissular portion which shows a low T2 Weighted Image and a low DWI can be considered as a benign [26].

Concerning ADC values, several previous studies showed that the mean ADC values for the solid portion of malignant tumors were significantly lower than in benign tumors [14] [12] which is consistent with our results. But others showed that the mean ADC values of the solid portion in malignant ovarian lesions did not significantly differ from benign lesions [8] [27]. This discrepancy was due to differences between studies conception. For instance, Takeuchi and al [14] have excluded endometriomas and mature teratomas which have a low ADC values (due respectively to hemorrhage or keratinoid components). Besides no significant difference have been showed between malignant and benign lesions because of certain types of solid benign tumors, such as fibromas, Brenner tumors, and cystadenofibromas, are known to be composed of tissues with a high number of collagen producing fibroblastic cells and a dense network of collagen fibers within the extracellular matrix which are likely to be associated with smaller ADC values [8]. In our study, despite the fact we included a lot of « fibrous » tumors (29 cystadenofibromas, 3 Brenner tumors) and mature teratomas, we could observe a difference in several ADC values between malignant and benign masses.

This could be thanks to the size of our sample (240 lesions) which is greater than in Takeuchi or Thomassin study (respectively 49 and 77 lesions).

In a study performed by Mimura and al [28], they demonstrate that minimum, mean, 10th, 25th, 50th, and 75th percentile ADC values of solid components of borderline tumors were significantly higher than in malignant tumors. In their study, the best parameter to distinguish borderline from malignant lesions was the 10th percentile with a high specificity (93.8%). No benign lesion was included in their study. In our study, we compared non-invasive (which include benign and borderline lesions) and invasive lesions and the best parameter to discriminate both lesions was the maximum ADC value from the hotspot ROI.

Finally, we demonstrate that a lower maximum ADC was associated to invasive compared to non-invasive and to malignant compared to benign lesions but with a relative low specificity and sensitivity. Furthermore, a $PLR_{Invasiveness} = 2.65$ and $PLR_{Malignancy}=2.07$ was respectively found, that implies that a low maximum ADC value increased moderately the probability for invasiveness or malignancy (a PLR between 2 and 3 change probability for the disease from 15 to 20%) [29]. Even in the particular sub-group of lesions rated A_{DNEX}MR Score 4 or 5, the $PLR_{Invasiveness}$ is up to 3.3.

Our study have several limitations. First of all, there was an heterogeneity in ADC measurements coming from acquisition from 1.5 or 3T MRI, and different b-values ($b=1000$ or $b=2000$) which is a source of heterogeneity [30]. Then, a small proportion of borderline tumors is represented in our population, that might underestimate our capacity to distinguish borderline from malignant tumors. Third, we did not perform a reproducibility assessment for the hotspot and the larger area ROI between 2 or more

readers. Especially for the larger ROI, it is not always easy to define the boundaries of the tissular portion, and artifacts or surrounding cystic components could influence the ADC value [31]. An other limitation was also to evaluate the ADC value on a 2 Dimension slice which could avoid some area from the tissular portion which could influence the ADC measurement.

In conclusion, we demonstrated that an ovarian tumors with a tissular portion with a low maximum ADC is more likely to be malignant (invasive and borderline) or invasive tumors. This trends is accentuated when the tumor is rated A_{DNEX}MR Score 4 or 5. But this is not accurate enough to distinguish malignant from borderline or invavise from non-invasive without using morphological and contrast-enhancement sequence.

REFERENCES

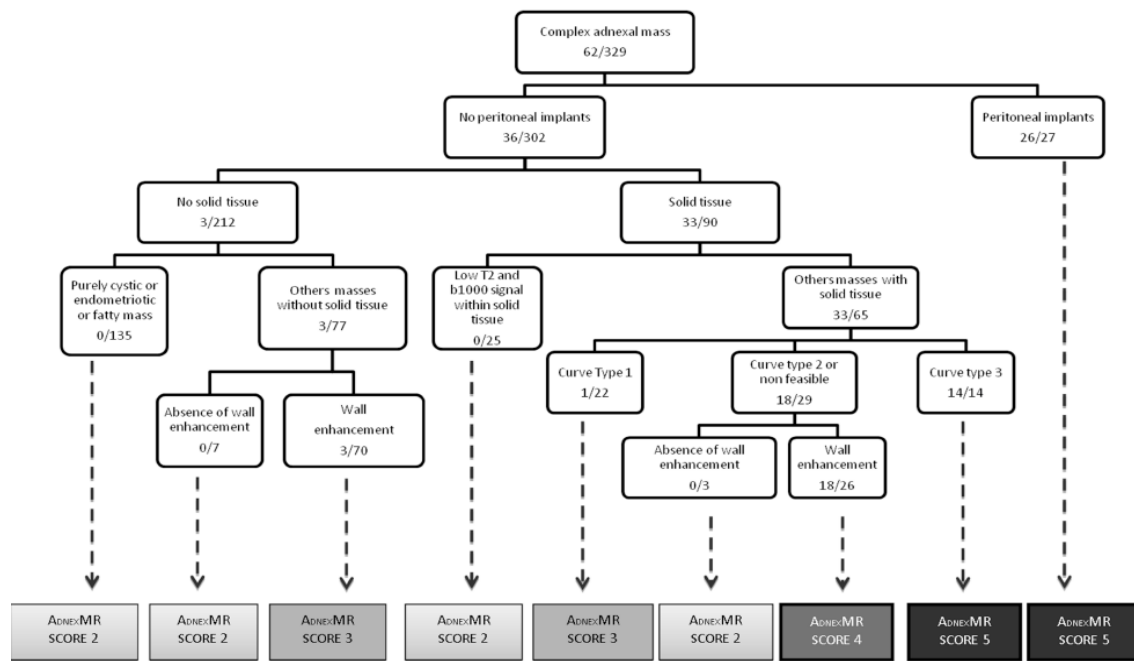
- [1] Curtin JP. Management of the adnexal mass, *Gynecol Oncol* 1994;55(3 Pt 2):S42-S46
- [2] Le Page C, Provencher D, Maugard CM, Ouellet V, Mes-Masson A-M. Signature of a silent killer: expression profiling in epithelial ovarian cancer. *Expert Rev Mol Diagn.* 2004;4(2):157–167
- [3] Bristow RE, Chang J, Ziogas A, Campos B, Chavez LR, Anton-Culver H. Impact of National Cancer Institute Comprehensive Cancer Centers on ovarian cancer treatment and survival. *J Am Coll Surg.* 2015;220(5):940–950.
- [4] Gynecologic sonography: report of the ultrasonography task force. Council on Scientific Affairs, American Medical Association. *JAMA* 1991;265(21):2851–2855.
- [5] Kinkel K, Lu Y, Mehdizade A, Pelte MF, Hricak H. Indeterminate ovarian mass at US: incremental value of second imaging test for characterization—meta-analysis and Bayesian analysis. *Radiology* 2005;236(1):85–94.
- [6] Hricak H, Chen M, Coakley FV, et al. Complex adnexal masses: detection and characterization with MR imaging—multivariate analysis. *Radiology* 2000;214(1):39–46.
- [7] Sohaib SA, Sahdev A, Van Trappen P, Jacobs IJ, Reznek RH. Characterization of adnexal mass lesions on MR imaging. *AJR Am J Roentgenol* 2003;180(5):1297–1304.
- [8] Thomassin-Naggara I, Toussaint I, Perrot N, et al. Characterization of complex adnexal masses: value of adding perfusion- and diffusion-weighted MR imaging to conventional MR imaging. *Radiology*. 2011;258(3):793–803.
- [9] Bernardin L, Dilks P, Liyanage S, Miquel ME, Sahdev A, Rockall A. Effectiveness of semi-quantitative multiphase dynamic contrast-enhanced MRI as a predictor of malignancy in complex adnexal masses: radiological and pathological correlation. *Eur Radiol* 2012;22(4):880–890.
- [10] Dilks P, Narayanan P, Reznek R, Sahdev A, Rockall A. Can quantitative dynamic contrast-enhanced MRI independently characterize an ovarian mass? *Eur Radiol* 2010;20(9):2176–2183.
- [11] Thomassin-Naggara I, Aubert E, Rockall A, et al. Adnexal masses: development and preliminary validation of an MR imaging scoring system. *Radiology*. 2013;267(2):432–443.
- [12] Li W, Chu C, Cui Y, et al. Diffusion-weighted MRI: a useful technique to discriminate benign versus malignant ovarian surface epithelial tumors with solid and cystic components. *Abdom Imaging* 2012;37:897–903.
- [13] Zhao SH, Qiang JW, Zhang GF, et al. Diffusion weighted MR imaging for differentiating borderline from malignant epithelial tumours of the ovary: pathological correlation. *Eur Radiol* 2014;24:2292–2299.

- [14] Takeuchi M, Matsuzaki K, Nishitani H. Diffusion-weighted magnetic resonance imaging of ovarian tumors: differentiation of benign and malignant solid components of ovarian masses. *J Comput Assist Tomogr* 2010;34(2):173–176.
- [15] Kurata, Yasuhisa & Kido, Aki & Moribata, Yusaku & Kameyama, Kyoko & Himoto, Yuki & Minamiguchi, Sachiko & Konishi, Ikuo & Togashi, Kaori. (2016). Diagnostic performance of MR imaging findings and quantitative values in the differentiation of seromucinous borderline tumour from endometriosis-related malignant ovarian tumour. *European Radiology*. 27. 10.1007/s00330-016-4533-x.
- [16] Timmerman D, Valentin L, Bourne TH, et al. Terms, definitions and measurements to describe the sonographic features of adnexal tumors: a consensus opinion from the International Ovarian Tumor Analysis (IOTA) Group. *Ultrasound Obstet Gynecol Off J Int Soc Ultrasound Obstet Gynecol*. 2000;16(5):500–505.
- [17] Thomassin-Naggara I, Daraï E, Cuenod CA, Rouzier R, Callard P, Bazot M. Dynamic contrast-enhanced magnetic resonance imaging: a useful tool for characterizing ovarian epithelial tumors. *J Magn Reson Imaging JMRI*. 2008;28(1):111–120.
- [18] Landis JR, Koch GG. The measurement of observer agreement for categorical data. *Biometrics*. 1977;33(1):159–174.
- [19] Guo AC, Cummings TJ, Dash RC, Provenzale JM (2002) Lymphomas and high-grade astrocytomas: comparison of water diffusibility and histologic characteristics. *Radiology* 224(1):177–183
- [20] Sugahara T, Korogi Y, Kochi M, Ikushima I, Shigematsu Y, Hirai T, Okuda T, Liang L, Ge Y, Komohara Y, Ushio Y, Takahashi M (1999) Usefulness of diffusion-weighted MRI with eco-planar technique in the evaluation of cellularity in gliomas. *J Magn Reson Imaging* 9(1):53–60
- [21] Coats JS, Freeberg A, Pajela EG, Obenous A, Ashwal S. Meta-analysis of apparent diffusion coefficients in the newborn brain. *Pediatr Neurol*. 2009; 41(4):263–74. Epub 2009/09/15. doi: 10.1016/j.pediatrneurol.2009.04.013 PMID: 19748046.
- [22] Thoeny HC, De Keyzer F. Extracranial applications of diffusion-weighted magnetic resonance imaging. *Eur Radiol*. 2007; 17(6):1385–93. Epub 2007/01/09. doi: 10.1007/s00330-006-0547-0 PMID: 17206421.
- [23] Bazot M, Daraï E, Nassar-Slaba J, et al. Value of magnetic resonance imaging for the diagnosis of ovarian tumors: a review. *J Comput Assist Tomogr*. 2008;32:712Y723.
- [24] Koyama T, Togashi K. Functional MR imaging of the female pelvis. *J Magn Reson Imaging*. 2007;25:1101Y1112.
- [25] Namimoto T, Awai K, Nakaura T, et al. Role of diffusion-weighted imaging in the diagnosis of gynecological diseases. *Eur Radiol*. 2009;19:745Y760.
- [26] Thomassin-Naggara I, Daraï E, Cuenod CA, et al. Contribution of diffusion-weighted MR imaging for predicting benignity of complex adnexal masses. *Eur Radiol*. 2009;19:1544Y1552.

- [27] Fujii S, Kakite S, Nishihara K, Kanasaki Y, Harada T, Kigawa J, et al. Diagnostic Accuracy of Diffusion-Weighted Imaging in Differentiating Benign From Malignant Ovarian Lesions. *J Magn Reson Imaging*. 2008;28(5):1149–56.
- [28] Mimura, R., Kato, F., Tha, K.K. et al. *Jpn J Radiol* (2016) 34: 229. Comparison between borderline ovarian tumors and carcinomas using semi- automated histogram analysis of diffusion- weighted imaging: focusing on solid components <https://doi.org/10.1007/s11604-016-0518-6>
- [29] McGee, S. *J GEN INTERN MED* (2002) 17: 647. <https://doi.org/10.1046/j.1525-1497.2002.10750.x>
- [30] Shan Pi, Rong Cao, Jin Wei Qiang, Yan Hui Guo, Utility of DWI with quantitative ADC values in ovarian tumors: a meta-analysis of diagnostic test performance *Acta Radiol*. 2018 Jan 1:284185118759708. doi: 10.1177/0284185118759708
- [31] Mukuda, N. , Fujii, S. , Inoue, C. , Fukunaga, T. , Tanabe, Y. , Itamochi, H. and Ogawa, T. (2016), Apparent diffusion coefficient (ADC) measurement in ovarian tumor: Effect of region-of-interest methods on ADC values and diagnostic ability. *J. Magn. Reson. Imaging*, 43: 720-725. doi:10.1002/jmri.25011.

ANNEXES

Annexe 1: ADNEX MR Score (From Thomassin-Naggara et al.Radiology 2012)



	<i>PLR</i>
ADNEXMR SCORE 1: No mass	-
ADNEXMR SCORE 2 : Benign mass Purely cystic mass Purely endometriotic mass Purely fatty mass Absence of wall enhancement Low b1000 and low T2-weighted signal intensity within solid component	0
ADNEXMR SCORE 3: Probably benign mass Curve type 1 within solid tissue Masses without solid tissue (except purely cystic, endometriotic and fatty mass)	<0.01
ADNEXMR SCORE 4: Indeterminate MR mass Curve type 2 within solid tissue	0.1-10
ADNEXMR SCORE 5 : Probably malignant mass Peritoneal implants Curve type 3 within solid tissue	>10

* Only one feature enough to classify in each category

Annexe 2 : Lexicon

Terms	Definitions
Purely cystic mass	Absence of internal enhancement after injection and corresponded a to unilocular cyst or hydrosalpinx, both of which have low T1--weighted and high T2---weighted MR signal intensities.
Purely endometriotic mass	Lesion displaying high T1---weighted signal intensity greater or equal to subcutaneous fat, shading on T2---weighted MR sequence and no internal enhancement.
Fatty mass without enhanced component	Lesion displaying high T1---weighted signal intensity that disappeared after fat saturation and potentially displaying non--enhancing solid component
Wall enhancement	Enhancement of the wall of a cyst
Bi or multilocularity	A cyst that has two or more septa. A septum is defined as a thin strand of tissue running across the cyst cavity from one internal surface to the contralateral side.
Grouped septa	A cyst contains grouped septae if 3 or more septa are close together in a part of the cyst.
Thickened regular septa	A smooth septation with a thickness > or equal to 3mm within a cystic tissue.
Solid tissue	As defined by IOTA group, solid tissue displays a positive Doppler flow. Thus, using MR imaging, a solid tissue enhances after gadolinium injection. In adnexal tumors, diffuse wall thickening, normal ovarian stroma and regular septa are not regarded as solid tissue according to IOTA group. Thus, solid tissue is either thickened irregular septa, and/or vegetation and/or solid portion (including completely solid mass).
Solid papillary projections	Defined by IOTA group as any solid projections into the cyst from the cyst wall with height greater or equal to 3mm.
Mixed or purely solid mass	= Solid nodule defined by IOTA group as any solid tissue which is not a wall, a septum or a vegetation. This group comprises completely solid masses.
Thickened irregular septa	Focal areas of septal thickening with a thickness > or equal to 3 mm within a cystic tissue.
T2---weighed signal intensity within solid tissue	Signal intensity defined in comparison with adjacent external myometrium.
b ₁₀₀₀ ---weighted signal intensity within solid tissue	Signal intensity defined in comparison with serous fluid (i.e., urine in bladder or cerebrospinal fluid[CSF])
Time intensity curve with solid tissue type 1	A gradual increase in the signal of the solid tissue, without a well-defined shoulder.
Time intensity curve within solid tissue type 2	A moderate initial rise in the signal of solid tissue relative to that of myometrium.
Time intensity curve within solid tissue type 3	An initial rise in the signal of solid tissue that was steeper than that of myometrium.

Ascites	Fluid in peritoneal cavity.
Peritoneal implants	Nodular thickening of the peritoneum that enhances after gadolinium injection.
<i>From Thomassin---Naggara et al. Radiology 2012 in press</i>	

Vu, le Directeur de Thèse



Vu, le Doyen
De la Faculté de Médecine de Tours
Tours, le

BRAULT Antoine

50 pages – 6 tableaux – 1 figures – 2 illustrations

Résumé :

Objectif: Evaluer les différents paramètres ADC issus d'une région d'intérêt localisée et d'une région d'intérêt occupant la plus grande partie possible de la portion solide de tumeurs ovariennes bénignes, frontières et malignes. Nous avons également essayé d'associer une valeur quantitative issue de la cartographie ADC au Score ADNEX-MR pour prédire le potentiel invasif d'une tumeur ovarienne.

Matériels et méthodes: 194 femmes (âge médian de 53,5 ans, de 18 à 95 ans) représentant 240 lésions ovariennes ont été incluses dans notre étude. 2 régions d'intérêt (une localisée et une la plus grande possible) étaient placées dans la portion tissulaire des masses annexielles. Les valeurs moyennes, minimales, maximales, la deviation standard pour les 2 régions d'intérêt ont été calculées pour les différentes lésions ainsi que les 5ème, 10ème, 20ème, 50ème, 75ème et 95ème percentiles pour la plus grande région d'intérêt et comparées aux constatations anatomopathologiques et le suivi à 2 ans.

Résultats: Les valeurs d'ADC moyennes, minimales et maximales sont significativement plus faibles dans les tumeurs invasives que dans les tumeurs frontières et bénignes quelque soit le type de région d'intérêt utilisé. La valeur maximale du hotspot est la plus discriminante.

Mots clés : Tumeurs ovariennes, diffusion, coefficient ADC, masses, caractérisation

Jury :

Président du Jury : Professeur Laurent BRUNEREAU

Directeur de thèse : Professeur Isabelle THOMASSIN-NAGGARA

Membres du Jury : Professeur Frédéric PATAT
: Docteur Aurore BLEUZEN

:

: Date de soutenance : 30/10/2018